J|A|C|S
ARTICLES
Published on Web 01/23/2008

Fluorinated Porphyrin Tweezer: A Powerful Reporter of Absolute Configuration for *erythro* and *threo* Diols, Amino Alcohols, and Diamines

Xiaoyong Li, Marina Tanasova, Chrysoula Vasileiou, and Babak Borhan*

Department of Chemistry, Michigan State University, East Lansing, Michigan 48824

Received July 14, 2007; E-mail: babak@chemistry.msu.edu

Abstract: A general and sensitive nonempirical protocol to determine the absolute configurations of *erythro* and *threo* diols, amino alcohols, and diamines is reported. Binding of diols to the porphyrin tweezer system is greatly enhanced by increasing the Lewis acidity of the metalloporphyrin. Supramolecular complexes formed between the porphyrin tweezer host and chiral substrates exhibited exciton-coupled bisignate CD spectra with predictable signs based on the substituents on the chiral center. The working model suggests that the observed helicity of the porphyrin tweezer is dictated via steric differentiation experienced by the porphyrin ring bound to each chiral center. A variety of *erythro* and *threo* substrates were investigated to verify this chiroptical method. Their absolute configurations were unequivocally determined, and thus a general mnemonic is provided for the assignment of chirality.

Introduction

Vicinal substituted heterofunctionalized chiral molecules such as *erythro* and *threo* diols, amino alcohols, and diamines are widely present in biologically active natural and synthetic products such as alkaloids, polyketides, and carbohydrates. They also play a crucial role in asymmetric catalysis, functioning as fundamental building blocks or chiral auxiliaries and ligands. The biological or catalytic activity of this class of compounds is often governed by their configurations. Consequently, development of methods to determine their absolute stereochemistry has been an active area of research.

For the most part, the absolute stereochemical determination of *threo* substituted systems can be achieved with the implementation of the dibenzoate methodology.[1−3] This is accomplished via derivatization of the functional groups with benzoates (or other similar chromophores),[4−15] which enables the absolute stereochemical determination of the chiral molecule based on the observed Exciton Coupled Circular Dichroism (ECCD).[1,2] Nonetheless, the need for derivatization is not ideal. The absolute stereochemistry of *erythro* systems, however, cannot be reliably assigned via existing strategies and remains a challenging and largely unresolved issue.

Briefly, the ECCD method relies on the coupling of the electric transition dipole moments of two or more chromophores held in space in a chiral fashion.[1] The sign of the resultant ECCD couplet reflects the helicity of the interacting chromophores and consequently the chirality of the derivatized system (see Figure 1, dashed box). The challenge in utilizing ECCD for absolute stereochemical determinations is not only to orient two or more chromophores in a chiral fashion dictated strictly by the chiral center but also to arrive at a system robust enough that it provides consistent results with structurally different compounds. Figure 1 illustrates the dibenzoate method for *threo* and *erythro* diols. With *threo* diols, the expected high population (low energy) rotomer leads to an observable and distinct ECCD spectrum. For the *threo* diol depicted in Figure 1, the result is a positive ECCD irrespective of R_1 and R_2. The expected high population rotomer for derivatized *erythro* diols, however, is ECCD silent. The expected minor populations lead to opposing ECCD spectra and thus cannot be used as a reliable indicator of absolute stereochemistry.

Other approaches have been developed to transform acyclic substrates into cyclic conformationally defined derivatives through generation of cottonogenic derivatives with metal

(1) Harada, N.; Nakanishi, K. *Circular Dichroic Spectroscopy: Exciton Coupling in Organic Stereochemistry*; University Science Books: Mill Valley, CA, 1983.
(2) Berova, N.; Nakanishi, K.; Woody, R. W. *Circular Dichroism: Principles and Applications*, 2nd ed.; Wiley-VCH: New York, 2000.
(3) Kawamura, A.; Berova, N.; Nakanishi, K.; Voigt, B.; Adam, G. *Tetrahedron* **1997**, *53*, 11961−11970.
(4) Wiesler, W. T.; Nakanishi, K. *J. Am. Chem. Soc.* **1989**, *111*, 9205−9213.
(5) Uzawa, H.; Nishida, Y.; Ohrui, H.; Meguro, H. *J. Org. Chem.* **1990**, *55*, 116−122.
(6) Harada, N.; Saito, A.; Ono, H.; Gawronski, J.; Gawronska, K.; Sugioka, T.; Uda, H.; Kuriki, T. *J. Am. Chem. Soc.* **1991**, *113*, 3842−3850.
(7) Zhou, P.; Zhao, N.; Rele, D. N.; Berova, N.; Nakanishi, K. *J. Am. Chem. Soc.* **1993**, *115*, 9313−9314.
(8) Zhou, P.; Berova, N.; Wiesler, W. T.; Nakanishi, K. *Tetrahedron* **1993**, *49*, 9343−9352.
(9) Cai, G. L.; Bozhkova, N.; Odingo, J.; Berova, N.; Nakanishi, K. *J. Am. Chem. Soc.* **1993**, *115*, 7192−7198.
(10) Matile, S.; Berova, N.; Nakanishi, K.; Novkova, S.; Philipova, I.; Blagoev, B. *J. Am. Chem. Soc.* **1995**, *117*, 7021−7022.
(11) Zhao, N.; Berova, N.; Nakanishi, K.; Rohmer, M.; Mougenot, P.; Jurgens, U. J. *Tetrahedron* **1996**, *52*, 2777−2788.
(12) Matile, S.; Berova, N.; Nakanishi, K.; Fleischhauer, J.; Woody, R. W. *J. Am. Chem. Soc.* **1996**, *118*, 5198−5206.
(13) Rele, D.; Zhao, N.; Nakanishi, K.; Berova, N. *Tetrahedron* **1996**, *52*, 2759−2776.
(14) Jiang, H.; Huang, X. F.; Nakanishi, K.; Berova, N. *Tetrahedron Lett.* **1999**, *40*, 7645−7649.
(15) Weckerle, B.; Schreier, P.; Humpf, H. U. *J. Org. Chem.* **2001**, *66*, 8160−8164.

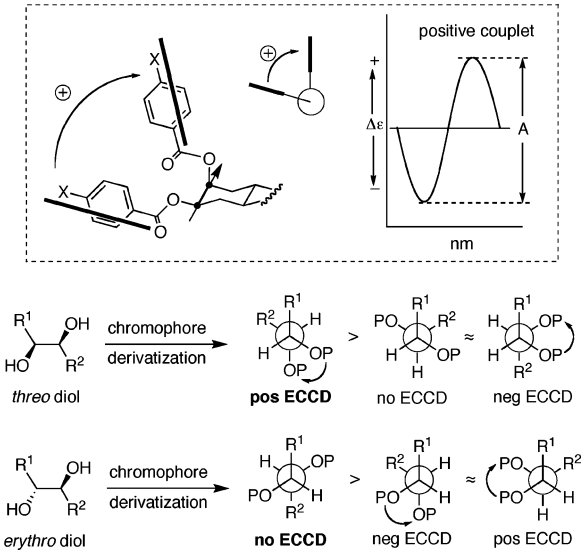

Figure 1. Excitonic coupling of two chromophores leads to an observable ECCD, the sign of which reflects the helicity of the coupling chromophores (dashed box). The major rotomer of derivatized *threo* diols leads to an observable ECCD spectrum. The major rotomer of derivatized *erythro* diols is ECCD silent.

complexes[16−24] or conversion into dioxolanes[25−28] or 4-biphenylborates.[29,30] These methods, however, suffer from fairly weak CD signals due to weak effective transition moments of the cottonogenic species, and few address the absolute stereochemical determination of *erythro* compounds. A practical and universally expedient method to unequivocally determine the chirality of *erythro* diols, amino alcohols, and diamines is a challenging task.

Porphyrin tweezer systems (Figure 2a) have been successfully used to determine the stereochemistry of chiral amines,[31−33] alcohols,[32,34] and carboxylic acids.[35−37] The principle advantage of the porphyrin tweezer system resides with the noncovalent

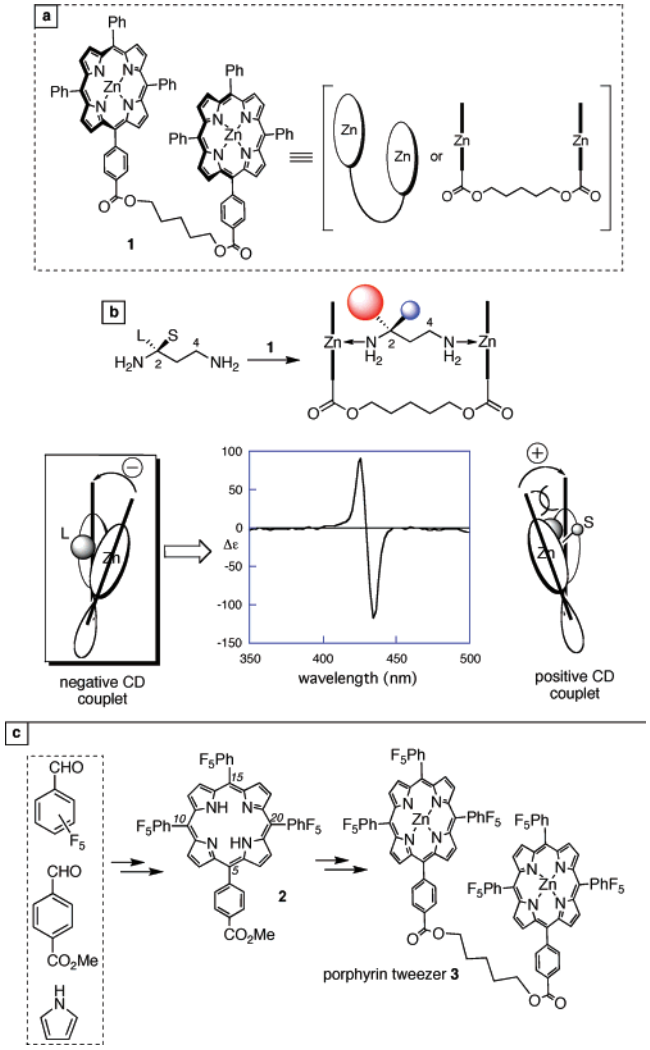

Figure 2. (a) Structure of Zn−TPP tweezer **1**. (b) Binding of a chiral diamine to **1** leads to a helical disposition of the porphyrin rings dictated by the sterics at the chiral center. The resultant ECCD is used to assign the absolute stereochemistry of the chiral center. (c) Structure and synthesis of Zn-TPFP tweezer **3**.

binding of the chiral guest, which precludes the need for chemical derivatizations. Prior work, however, has focused on the absolute stereochemical determination of single chiral centers. As depicted in Figure 2b, the binding of the Zn-porphyrin tweezer to a diamine with a single chiral center leads to an induced helical arrangement of the bound porphyrins that yields a predictable ECCD spectrum.[31] Since the tweezer strategy is based on the steric interaction between the substituents at the chiral center and one of the two porphyrins, it was envisaged that the second porphyrin could participate in steric differentiation with chiral guests that have two chiral centers such as 1,2-bisfunctionalized systems. In other words, we hypothesized that a system with two chiral centers could be considered as two systems with a single chiral center each. In this manner, *erythro* diols, amino alcohols, and diamines could yield reproducible ECCD spectra based on the steric differentiation at each chiral center. We predict that the porphyrin would bind the hydroxyl group *anti* to the largest substituent on the chiral center and stereodifferentiate between the two remaining groups attached to the same chiral carbon. Upon steric differentiation at each chiral center, the two porphyrins would adopt a specific helicity. It should be noted that assuming a 1,2-

(16) Dillon, J.; Nakanishi, K. *J. Am. Chem. Soc.* **1975**, *97*, 5409−5417.
(17) Dillon, J.; Nakanishi, K. *J. Am. Chem. Soc.* **1975**, *97*, 5417−5422.
(18) Snatzke, G.; Wagner, U.; Wolff, H. P. *Tetrahedron* **1981**, *37*, 349−361.
(19) Frelek, J.; Snatzke, G. *Fresenius Z. Anal. Chem.* **1983**, *316*, 261−264.
(20) Frelek, J.; Ikekawa, N.; Takatsuto, S.; Snatzke, G. *Chirality* **1997**, *9*, 578−582.
(21) Frelek, J.; Geiger, M.; Voelter, W. *Curr. Org. Chem.* **1999**, *3*, 117−146.
(22) Di Bari, L.; Pescitelli, G.; Pratelli, C.; Pini, D.; Salvadori, P. *J. Org. Chem.* **2001**, *66*, 4819−4825.
(23) Scott, A. I.; Wrixon, A. D. *J. Chem. Soc., Chem. Commun.* **1969**, 1184−1186.
(24) Di Bari, L.; Lelli, M.; Pintacuda, G.; Salvadori, P. *Chirality* **2002**, *14*, 265−273.
(25) Rosini, C.; Scamuzzi, S.; Pisani-Focati, M.; Salvadori, P. *J. Org. Chem.* **1995**, *60*, 8289−8293.
(26) Superchi, S.; Casarini, D.; Laurita, A.; Bavoso, A.; Rosini, C. *Angew. Chem., Int. Ed.* **2001**, *40*, 451−454.
(27) Rosini, C.; Scamuzzi, S.; Uccellobarretta, G.; Salvadori, P. *J. Org. Chem.* **1994**, *59*, 7395−7400.
(28) Donnoli, M. I.; Scafato, P.; Superchi, S.; Rosini, C. *Chirality* **2001**, *13*, 258−265.
(29) Superchi, S.; Donnoli, M. I.; Rosini, C. *Org. Lett.* **1999**, *1*, 2093−2096.
(30) Superchi, S.; Casarini, D.; Summa, C.; Rosini, C. *J. Org. Chem.* **2004**, *69*, 1685−1694.
(31) Huang, X. F.; Rickman, B. H.; Borhan, B.; Berova, N.; Nakanishi, K. *J. Am. Chem. Soc.* **1998**, *120*, 6185−6186.
(32) Kurtan, T.; Nesnas, N.; Li, Y. Q.; Huang, X. F.; Nakanishi, K.; Berova, N. *J. Am. Chem. Soc.* **2001**, *123*, 5962−5973.
(33) Huang, X. F.; Fujioka, N.; Pescitelli, G.; Koehn, F. E.; Williamson, R. T.; Nakanishi, K.; Berova, N. *J. Am. Chem. Soc.* **2002**, *124*, 10320−10335.
(34) Lintuluoto, J. M.; Borovkov, V. V.; Inoue, Y. *J. Am. Chem. Soc.* **2002**, *124*, 13676−13677.
(35) Proni, G.; Pescitelli, G.; Huang, X. F.; Quraishi, N. Q.; Nakanishi, K.; Berova, N. *Chem. Commun.* **2002**, 1590−1591.
(36) Yang, Q. F.; Olmsted, C.; Borhan, B. *Org. Lett.* **2002**, *4*, 3423−3426.
(37) Proni, G.; Pescitelli, G.; Huang, X. F.; Nakanishi, K.; Berova, N. *J. Am. Chem. Soc.* **2003**, *125*, 12914−12927.

bisfunctionalized molecule as a system with two independent chiral sites is an oversimplification, since the conformation of the molecule would clearly play a large role in the overall helicity of the complexed porphyrin tweezer. Nevertheless, without a clear picture of the molecule's conformation upon complexation with the porphyrin tweezer, one can assume that the conformation adopted would be dictated by the fact that each chiral site is now complexed with a large porphyrin ring, and thus the overall conformation can be hypothesized by adopting a rotomer that minimizes interaction at each chiral center.

A problematic issue was the weak binding of alcoholic chiral guests with zinc porphyrin tweezers employed previously. For this approach to work, we required a strong binding tweezer such that a large population of the chiral guest (for example, 1,2-diols) would bind and, thus, increase the observed signal. Also, weak binding complexes could lead to small energetic differences between a number of complexed conformations. Inconsistent trends in observed ECCD are possible upon binding of different structures if different conformations yield opposite ECCD. In fact, we have observed a mix of positive and negative ECCD with different substrates that have the same chirality when weak binding tweezers were utilized. The latter criteria led to the design and synthesis of 5-(4-methylcarboxyphenyl)-10,15,20-tri(pentafluorophenyl) porphyrin (**2**, Figure 2c). The use of this electron-deficient porphyrin yields a Lewis acidic zincated porphyrin tweezer that binds diols strongly.

Herein, we demonstrate the utilization of an electron deficient zincated porphyrin tweezer as an effective host system for binding of 1,2-bisfunctionalized diols, amino alcohols, and diamines. Moreover, we disclose a routine and robust system for the absolute stereochemical determination of both *threo* and *erythro* systems without the need for chemical derivatization.

Results and Discussion

Synthesis of Tweezer 3 and Binding Affinity Measurements. Porphyrin **2** (Figure 2c) was synthesized using a modified literature procedure.[10] The zincated porphyrin tweezer **3** was prepared using protocols described previously (Figure 2c, $\lambda_{max} = 416$ nm, $\epsilon = 1\,120\,000$ cm^{-1} M^{-1} in CH_2Cl_2; $\lambda_{max} = 412$ nm, $\epsilon = 890\,000$ cm^{-1} M^{-1} in hexane).[31] Calculations, ^{1}H NMR binding experiments, and UV−vis titrations corroborate the enhanced Lewis acidity and binding affinity of the new fluorinated porphyrin.

Computational modeling was utilized to investigate the change in Lewis acidity of the zinc atom in the fluorinated porphyrin as compared to its nonfluorinated counterpart. Zinc 5-(4-methylcarboxyphenyl)-10,15,20-tri(pentafluorophenyl) porphyrin (Zn-TPFP-monoester, Table 1, **4**) and zinc 5-(4-methylcarboxyphenyl)-10,15,20-triphenyl porphyrin (Zn-TPP-monoester, Table 1, **5**) were used as model compounds. Geometry optimization was performed by the semiempirical method (PM3) followed by DFT single-point energy calculation at the B3LYP/6-31G(d) level of theory.

As shown in Table 1, the fluorinated porphyrin has a lower LUMO energy. This indicates an increased Lewis acidity as well as binding affinity toward nucleophilic guest molecules since the decreased LUMO energy would lead to a smaller energy gap between the LUMO of the electrophilic host and the HOMO of the nucleophilic guest. The calculated charges

Table 1. Frontier Orbital Energy and Charges of Zinc Porphyrins

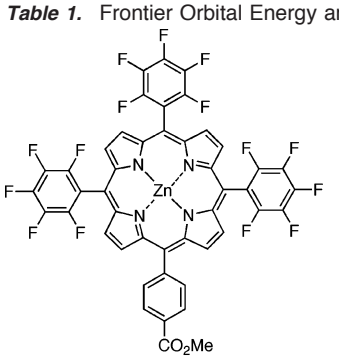

Zn-TPFP-ester, **4**

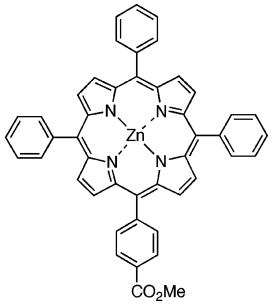

Zn-TPP-ester, **5**

	E_{LUMO} eV	$E_{LUMO} - E_{HOMO}$ eV[a]	Mulliken charge of Zn^{2+}	electrostatic charge of Zn^{2+}
Zn-TPFP-monoester	−2.818	3.284	0.961	1.387
Zn-TPP-monoester	−2.211	3.891	0.942	1.337

[a] *S*-Lysine methyl ester was chosen as a typical chiral guest. HOMO energy calculated using the same method was −6.102 eV.

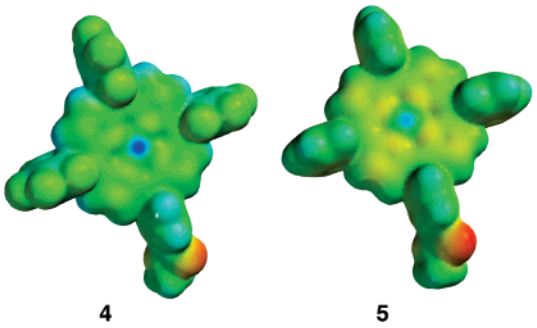

4 **5**

Figure 3. Electrostatic potential surface of Zn-TPFP-monoester (**4**) and Zn-TPP-monoester (**5**) based on B3LYP/6-31G(d)//PM3 calculation. Property range was set from −45 (red color) to +45 (blue color).

also provide evidence that the zinc atom bound to the Zn-TPFP-monoester (**4**) is more electropositive, presumably due to the strong electron-withdrawing effect of the pentafluorophenyl groups as compared to Zn-TPP-monoester (**5**). Electrostatic potential surfaces (Figure 3) provide a visual perspective of the charge difference between the two zinc porphyrins. The Zn-TPFP-monoester is clearly more electron deficient than the Zn-TPP-monoester as represented by the "colder" surface.

The enhanced binding could also be observed through ^{1}H NMR analysis. Binding of ethanol to zincated porphyrin **4** (1:1 ratio) led to a 0.5 ppm upfield shielding of the methylene protons. Ethanol bound to zincated tetraphenyl porphyrin **5** upfield shifted the methylene protons by only 0.1 ppm, clearly indicating a stronger binding affinity of porphyrin **4** with ethanol.

Quantitative measures of amine and alcohol binding with both Zn-TPP and Zn-TPFP were obtained via titration of the ligands and analysis of the spectroscopic changes. Zn-TPFP-ester **4** and Zn-TPP-ester **5** were used as simplified models of each tweezer for initial measurements. Figure 4 illustrates the changes observed in the UV−vis spectra upon titration of isopropanol and isopropylamine with Zn−TPFP-ester **4**. The change of absorption at 418 nm for isopropanol and 412 nm for isopropylamine as a function of concentration of ligand added yields an exponential saturation curve. The binding constants can be derived from fitting the latter data via a nonlinear least-squares

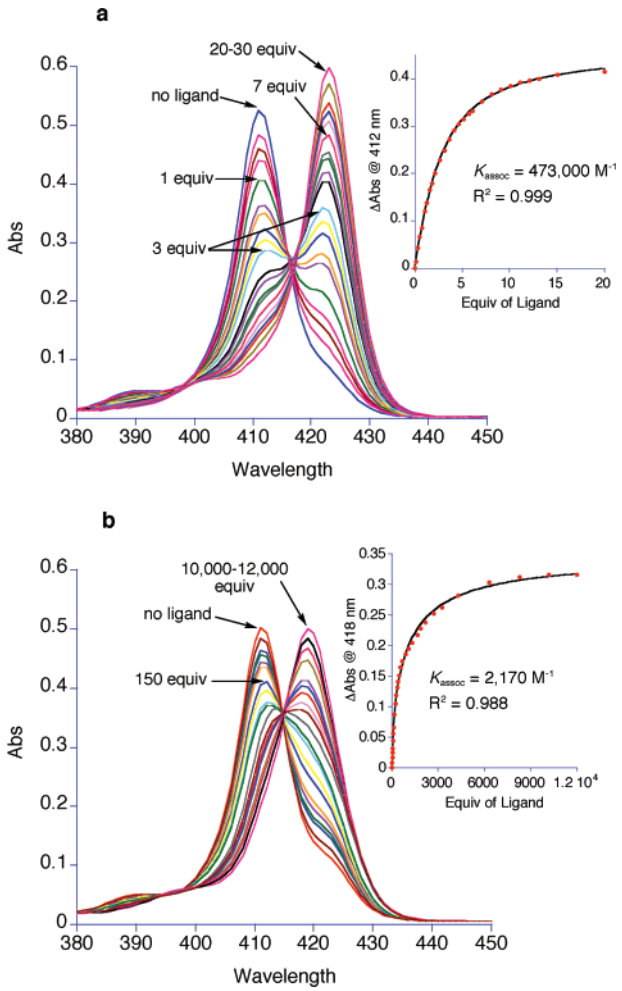

Figure 4. Titration of Zn-TPFP ester **4** with (a) *i*PrNH$_2$ (0−30 equiv, bathochromic shift from 412 to 424 nm) and (b) *i*PrOH (0−12 000 equiv, bathochromic shift from 412 to 418 nm) in hexane. Both systems exhibit a bathochromic shift upon addition of ligand. The inset graphs are nonlinear least-squares fits of the change in absorption vs equiv of ligand for each.

Table 2. Binding Affinity of *i*PrOH and *i*PrNH$_2$ with Zn-TPP-Ester and Zn-TPFP-Ester[a]

porphyrin	K_{assoc} (*i*PrOH) M^{-1}	K_{assoc} (*i*PrNH$_2$) M^{-1}
Zn-TPFP-monoester (**4**)	2170 ± 140	473 000 ± 8700
Zn-TPP-monoester (**5**)	49 ± 2	11 400 ± 950

[a] K_{assoc} for each ligand/porphyrin complex was obtained via fitting the data obtained from the change in the absorption upon titration of the porphyrin with ligand in hexane to a nonlinear least-squares analysis routine described in the Supporting Information.

method as has been previously reported.[38] Table 2 lists the binding constants obtained for Zn-TPFP-ester **4** and Zn-TPP-ester **5**. As expected, isopropylamine binds more strongly to the Zn-porphyrins as compared to isopropanol. Of note, however, is a greater than 1 order of magnitude increase in binding affinity of the ligands (both amine and alcohol) for the fluorinated Zn-porphyrin **4** as compared to the nonfluorinated Zn-porphyrin **5**.

We next turned our attention to the binding of bis-functionalized substrates with the Zn-porphyrin tweezers derived from TPP-ester and TPFP-ester. Figure 5 illustrates the binding

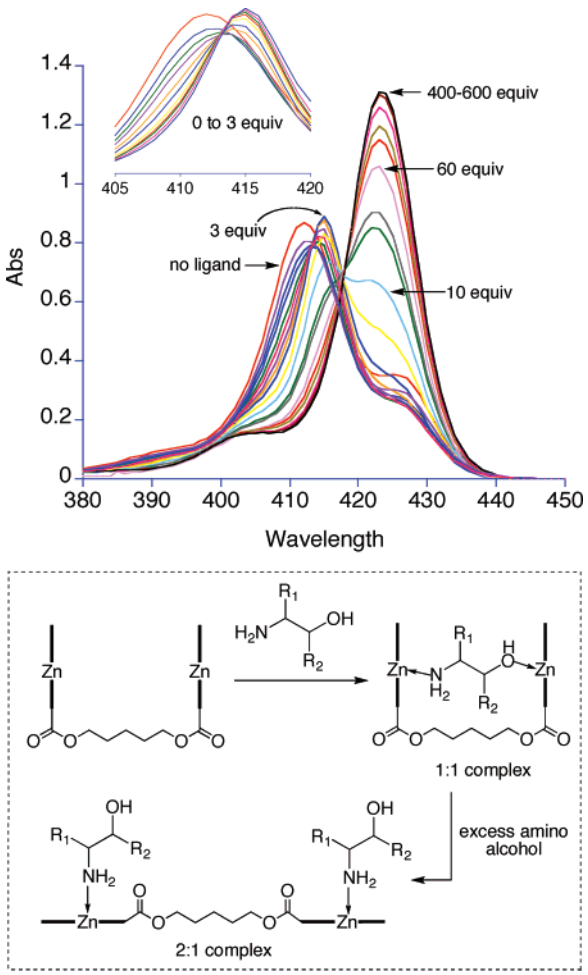

Figure 5. Titration of Zn-TPFP-tweezer **3** with amino alcohol **12**. Two isosbestic points are apparent. The first at lower equivalence of amino alcohol (leading to the absorption at 415 nm) signifies the 1:1 ligand/complex formation. The second (leading to the absorption at 423 nm) appearing at higher concentrations of amino alcohol indicates the formation of the 2:1 ligand/tweezer complex (see dashed box).

titration of amino alcohol **12** with tweezer **3**. Close inspection of the UV−vis spectra reveals the presence of two processes as the concentration of the ligand is increased. From prior work it is well recognized that a ∼12 nm bathochromic shift is expected upon coordination of a strong nucleophile such as an amino group with the zinc porphyrin.[39] It has also been demonstrated previously that a hypsochromic shift occurs when the two porphyrin rings are brought close in space.[40] Thus, there are two opposing effects that in combination lead to the observed λ_{max}. For example, upon complexation of 1,2-diaminoethane, a 4 nm bathochromic shift is observed (as opposed to the expected 12 nm); as the separation between the porphyrin rings is increased the λ_{max} gradually redshifts such that binding of 1,-10-diaminodecane results in a 9 nm bathochromic shift.[40]

The titration curves depicted in Figure 5 exhibit an initial bathochromic shift of the absorption maximum from 412 to 415 nm when the first 3 equiv of the 1,2-amino alcohol **12** are added to tweezer **3** in hexane. As the equivalence is increased, however, a second bathochromic shift to 423 nm is evident.

(38) Shoji, Y.; Tashiro, K.; Aida, T. *J. Am. Chem. Soc.* **2006**, *128*, 10690−10691.
(39) Hunter, C. A.; Meah, M. N.; Sanders, J. K. M. *J. Am. Chem. Soc.* **1990**, *112*, 5773−5780.
(40) Huang, X.; Borhan, B.; Berova, N.; Nakanishi, K. *J. Indian Chem. Soc.* **1998**, *75*, 725−728.

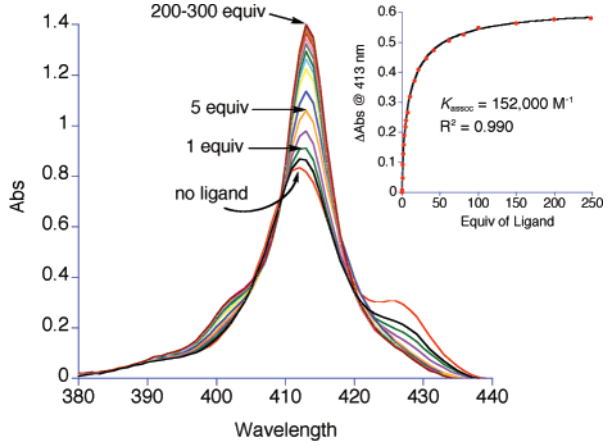

Figure 6. Titration of Zn-TPFP tweezer **3** with diol **16** (0−300 equiv) in hexane. The nonlinear least-squares fit of the change in absorption vs equiv of ligand provides the binding constant.

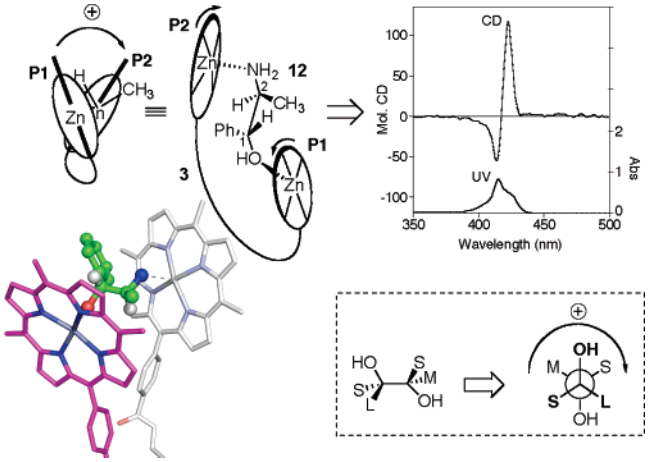

Figure 7. Proposed binding conformation between tweezer **3** and *erythro* amino alcohol **12**, yielding a positive ECCD spectrum. It is assumed that **P1** and **P2** bind to their respective functional groups opposite the large group at each chiral center. Thus **P1** binds the alcohol in an *anti* fashion with respect to the phenyl group and sterically differentiates between the smaller hydrogen group and C2. This results in a counterclockwise rotation of **P1**. In an analogous fashion, **P2** rotates in a clockwise manner, leading to an overall positive helicity of the tweezer and the observed ECCD spectrum. The model illustrates the proposed binding of tweezer **3** with amino alcohol **12** (the pentafluorophenyl groups in the modeled picture have been omitted for clarity). A simplified mnemonic is illustrated in the dashed box. The sign of the ECCD spectrum will depend only on the absolute stereochemistry of the chiral center that bears the largest group.

This behavior can be explained based on the observations discussed above; i.e., the initial 3 nm bathochromic shift is due to a 1:1 complexation of the 1,2-amino alcohol with tweezer **3**, which brings the porphyrins close to each other. This results in the observed 3 nm redshifting that gives rise to the peak at 415 nm. Further increase in the concentration of the 1,2-amino alcohol leads to the breakup of the 1:1 complex (binding of an amine to the zincated porphyrin is much stronger than that of an alcohol) such that each porphyrin is bound to an amino group (1:2 complex), effectively maximizing the distance between the porphyrin rings that leads to an 11 nm redshift. This is analogous to a monoamine binding to the porphyrin, which would result in the same level of redshifting. We would thus expect that excess addition of chiral 1,2-amino alcohols to the porphyrin tweezer would diminish the anticipated ECCD.

Based on the latter discussion, the binding constant for a 1:1 complexation of **12** with tweezer **3** was measured based on the data obtained for up to 3 equiv of amino alcohol added. Nonlinear least-squares analysis of the change in absorption at 412 nm as a function of guest concentration provided a binding constant (K_{assoc}) of 1.31×10^7 M^{-1} for binding of **12** with tweezer **3** in hexane. Similar UV titrations in methylcyclohexane (MCH) with guest **12** rendered a binding constant of 2.71×10^6 M^{-1}. The better binding in hexane might lead to stronger ECCD amplitudes.

As anticipated, the binding of 1,2-diols with tweezer **3** is weaker due to the tempered nucleophilicity of alcohols compared to amines. Figure 6 depicts the UV−vis titration curves of diol **16** complexed with tweezer **3** (K_{assoc} = 152 000 M^{-1} in hexane, 36 100 M^{-1} in MCH). Two observations are notable; first a large bathochromic shift is not present upon binding of the hydroxyl group with the zincated porphyrin. This is the result of two opposing effects, the anticipated 6 nm bathochromic shift as a result of alcohol binding with the zincated porphyrin (see Figure 4b for alcohol−porphyrin binding) and the hypsochromic shift that results from bringing the two porphyrins close to each other. Second, since addition of excess 1,2-diol does not compete with the 1:1 complexation (previously, excess amine competed with the hydroxyl bound porphyrin), breakup of the 1:1 complex is not apparent. Addition of excess 1,2-diol to tweezer **3** mimics addition of excess diamines to porphyrin tweezers, which does not exhibit the breakup of the 1:1 complex until ~500 equiv are added.[37]

Determination of Chirality of *erythro* Substrates. Our initial foray focused on the use of the fluorinated tweezer **3** with *erythro* diols and amino alcohols. As can be seen from Figure 7 and Table 3, the binding of the chiral *erythro* guests yielded a host−guest complex with observable ECCD couplets. A consistent and predictable trend is observed, where the *R*,*S* *erythro* compounds (the first stereochemical designation refers to the chiral site with the largest substituent as determined by *A*-values) give rise to positive ECCD, while the *S*,*R* *erythro* compounds produced negative ECCD spectra. The Cahn, Ingold, and Prelog stereochemical designation should be used with caution since priorities do not necessarily correlate with sterics as can be seen in **7**, an example of an *R*,*R*-*erythro* diol.

Figure 7 illustrates a conceptual model that suggests each chiral center orients the bound porphyrin through steric differentiation. This is illustrated with the binding of norephedrine **12** with tweezer **3**. We propose that **P2** approaches the amino group of *R*,*S*-norephedrine opposite to the largest substituent, in this case the methyl group. In this manner, the methyl group is *anti* to the complexed porphyrin and does not participate in the steric differentiation. The two remaining groups attached to C1, namely H and the C2, dictate the disposition of the bound porphyrin ring; as such **P2** rotates clockwise toward the smaller hydrogen atom. Similarly, binding of **P1** with the OH group places **P1** *anti* to the phenyl group attached to C1. Steric differentiation of the remaining substituents (H and C2) leads to the rotation of **P1** in a counterclockwise manner to reduce repulsion with the bulky C2 substituent. As described, **P1** adopts a clockwise (positive) helicity relative to **P2**, which would predict a positive ECCD spectrum. Indeed, as illustrated in Figure 7, the complexation of **12** with porphyrin tweezer **3** leads to the anticipated spectrum. This is a working model that fits the data and by no means is the only possible mode of binding

Table 3. Tweezer **3** Bound *erythro*-1,2-Diols and Amino Alcohols

	Erythro substrates[a]	Predicted sign	Solvent	λ nm, (Δε)	A
6[b],[c] *R,S*		+	MCH	420 (+24) 415 (-5)	+29
			Hexane	421 (+43) 411 (-15)	+58
6-*ent*[b],[c] *S,R*		-	MCH	421 (-8) 414 (+20)	-28
			Hexane	421 (-18) 414 (+34)	-52
7[d],[e] *R,R*		+	MCH	423 (+22) 414 (-9)	+31
			Hexane	420 (+90) 410 (-41)	+131
7-*ent*[d],[e] *S,S*		-	MCH	423 (-17) 413 (+18)	-35
			Hexane	423 (-72) 413 (+62)	-134
8[b],[c] *R,S*		+	MCH	420 (+24) 413 (-5)	+29
			Hexane	419 (+56) 409 (-9)	+65
8-*ent*[b],[c] *S,R*		-	MCH	420 (-13) 413 (+15)	-28
			Hexane	419 (-39) 410 (+27)	-66
9[b],[d] *S,R*	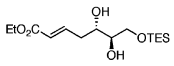	-	MCH	422 (-23) 414 (+25)	-48
			Hexane	420 (-43) 413 (+36)	-79
10[d],[e] *R,S*		+	MCH	422 (+13) 415 (-6)	+19
			Hexane	423 (+48) 409 (-16)	+64
11[e],[f] *S,R*		-	MCH	425 (-181) 416 (+114)	-295
			Hexane	425 (-341) 414 (+167)	-508
12[e],[f] *R,S*		+	MCH	423 (+92) 416 (-53)	+145
			Hexane	423 (+118) 414 (-56)	+174
12-*ent*[e],[f] *S,R*		-	MCH	423 (-93) 415 (+56)	-149
			Hexane	423 (-112) 414 (+65)	-177

[a] All substrates were >98% ee except for **10** (25% ee). [b] 2 μM tweezer concentration. [c] Tweezer/substrate ratio, 1:100. [d] Tweezer/substrate ratio, 1:40. [e] 1 μM tweezer concentration. [f] Tweezer/substrate ratio, 1:5.

(see Supporting Information for alternate binding conformation and molecular modeling studies).

Careful analysis of the results listed in Table 3 leads to a simplified mnemonic where the helicity of the tweezer can be determined by analyzing the chirality of one carbon center. Based on the proposal above, in which the two porphyrins (**P1** and **P2**) rotate counter to each other, one can consider solely the arrangement of **P1**, the porphyrin bound to the chiral center with the largest substituent, as the stereochemical determinant group (assuming the other porphyrin **P2** does not rotate and is static). As depicted in Figure 7 (dashed box) the stereochemistry of the chiral center with the largest substituent leads to the predicted ECCD; namely, looking at the Newman projection, a clockwise arrangement of S → OH → L leads to a positive ECCD and *vice versa*. This device should be used as a mnemonic for the given system and does not reflect the bound conformation of the chiral molecule.

As can be seen from Table 3, a number of alkyl and aryl systems produced the expected results upon binding with tweezer **3**. In all cases the predicted sign was arrived at after considering the *A*-values of the substituents on the carbinol carbon (the structures in Table 3 are drawn such that the larger group is on the left-hand side). The system is tolerant of other

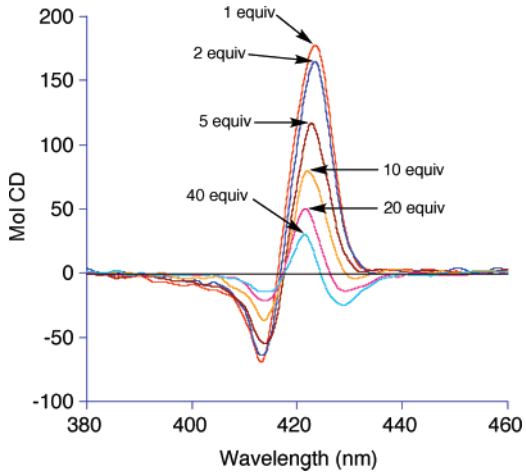

Figure 8. Increasing concentration of amino alcohol **12** leads to diminished ECCD signals. This is presumably a result of breaking up the ECCD active 1:1 ligand/tweezer complex (see Figure 5) due to the fact that amines have a much higher binding affinity for the zincated porphyrin. The resultant 2:1 complex is not ECCD active.

potential coordinating groups such as ketones, esters, and ethers (Table 3, compounds **7** and **9**). As expected, enantiomeric pairs yield opposite ECCD spectra (compounds **6**−**8** and **12** along with their enantiomers). Of note are the higher ECCD amplitudes obtained for amine containing guests **11** and **12**, which is presumably due to their stronger binding with tweezer **3** as compared to diols.

ECCD amplitudes of tweezer/guest complexes in hexane were consistently larger than those measured in MCH. This is most probably attributed to the observed stronger binding of 1,2-diols and 1,2-amino alcohols with tweezer **3** in hexane as compared to MCH. It seems reasonable that binding constants could be used as a guide for choosing the appropriate solvent in such cases. Other solvents such as dichloromethane or acetonitrile failed to yield observable ECCD for many substrates under the same conditions. Cooling of the solution to 0 °C produced strong observable ECCD spectra; however, further lowering of the temperature to −10 °C only led to a limited increase in the amplitude.

A note of caution is warranted with amino alcohols. As was eluded to above, the large difference in binding affinity of alcohols and amines with zincated porphyrins does lead to the breakup of the 1:1 complex with increasing equivalence of amino alcohols added. The resultant 2:1 complex is not ECCD active. Thus, increasing equivalence of amino alcohols is detrimental to obtaining a strong ECCD signal. Figure 8 demonstrates the decrease in signal as a function of increasing concentration of amino alcohol **12**, clearly suggesting the breakup of the 1:1 complex at higher equivalences.

Determination of Chirality for *threo* Substrates. Next we investigated *threo* vicinal bis-functionalized systems. Aliphatic and aromatic *R,R-threo* substrates yielded positive ECCD signals while the *S,S-threo* compounds produced negative ECCD spectra (Table 4). Seven pairs of *threo* enantiomers all exhibited mirror image CD couplets (see Supporting Information). Figure 9 illustrates the ECCD spectrum obtained from the complexation of tweezer **3** with the *threo* diol **13**. The expected positive couplet is again assumed to derive from steric differentiation of bound porphyrins at each chiral site. As depicted in Figure 9, each chiral center induces the same helical twist of the

Table 4. Tweezer **3**[a] Bound *threo*-1,2-Diols,[b] Amino Alcohols,[c] and Diamines[c]

	threo chiral substrates[d]	predicted sign	λ nm, (Δε)	A
13[e] *R,S*	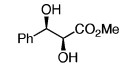	+	424 (+21) 415 (-16)	+37
14[e] *R,R*		+	422 (+25) 412 (-8)	+33
15[e] *R,R*		+	424 (+75) 413 (-30)	+105
16[e] *R,R*	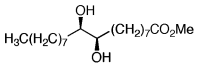	+	426 (+118) 413 (-33)	+151
17 *S,S*	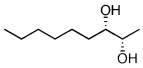	-	426 (-25) 412 (+16)	-41
18 *S,S*	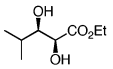	+	423 (+16) 412 (-4)	+20
19 *S,S*	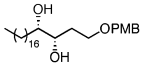	-	427 (-29) 415 (+12)	-41
20 *S,S*		-	423 (-27) 417 (+23)	-50
21 *R,R*	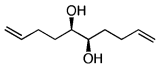	+	425 (+37) 414 (-17)	+54
22[e],[f] *S,S*	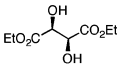	+	423 (+37) 414 (-22)	+59
23 *R,R*	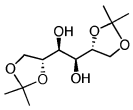	+	420 (+47) 412 (-21)	+68
24 *S,S*	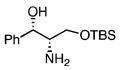	-	426 (-54) 421 (+35)	-89
25[e] *S,S*		-	428 (-41) 420 (+31)	-72
26[e] *R,R*		+	430 (+222) 419 (-142)	+364
27[b] *S,S*		+	420 (+39) 410 (-15)	+54

[a] 1 μM tweezer concentration was used for all measurements except for **19** and **27** (2 μM). [b] Tweezer/substrate ratio, 1:40. [c] Tweezer/substrate ratio, 1:5. [d] All substrates were >95% ee except for **15** and **27** (91% ee). [e] The enantiomer showed mirror image CD spectrum. [f] Tweezer/substrate ratio, 1:200, methyl cyclohexane was used as solvent for all CD measurements.

porphyrin tweezer (**P1** and **P2** twist counter to each other as indicated by the two arrows). As was described for *erythro* systems, we assume that the complexed porphyrins approach their ligands such that the largest group on the chiral center is *anti* with respect to the bound chromophores. The conformation illustrated for *threo* diol **13** in Figure 9, where the large groups (Ph on C1 and CO_2Me on C2) are placed *anti* to each other (similar to the conformation assumed for *erythro* systems), leads to the least sterically encumbered arrangement for the bound porphyrins. Steric differentiation at **P1** (H vs C2) leads to a counterclockwise rotation of the porphyrin toward the smaller hydrogen atom, while a clockwise rotation of **P2** (steric differentiation of H vs C1) is anticipated. This would lead to a positive helical arrangement of the porphyrins, which is verified by the positive ECCD spectrum observed for diol **13** bound to porphyrin tweezer **3**. Each stereocenter of a *threo* system would thus reinforce the same overall helicity of the bound tweezer.

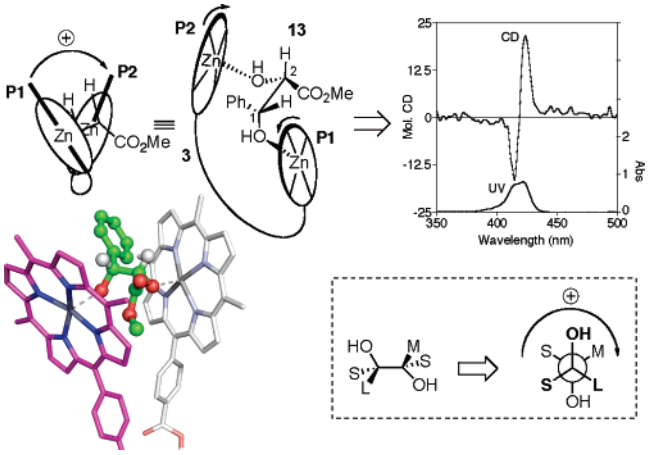

Figure 9. Proposed conformation of the complex generated between the binding of tweezer **3** (two arrows indicate the directions which the porphyrins would rotate to minimize steric repulsion) and *threo* diol **13**, resulting in a positive ECCD spectrum. The depicted arrangement is arrived at by placing **P1** and **P2** opposite the large group at each chiral center. Steric differentiation at each chiral center leads to the anticipated positive helical arrangement of the porphyrin rings (similar to the *erythro* case, **P1** rotates in a counterclockwise manner to avoid interactions with C2 in preference for the smaller hydrogen atom). The model illustrates the binding of diol **13** with tweezer **3** (the pentafluorophenyl groups have been omitted for clarity). The dashed box depicts a simplified mnemonic for the absolute stereochemical determination of *threo* systems based on analysis of the chiral center with the largest substituent.

The latter statement would suggest that C_2 symmetric diols and diamines would lead to observable ECCD spectra. This is indeed observed (Table 4, compounds **20**−**23** and **26**−**27**) making this methodology applicable to the absolute stereochemical identification of C_2 symmetric compounds, which are an important subgroup of chiral molecules used in various enantioselective processes. The same simplified mnemonic that was used for *erythro* systems is applicable for *threo* compounds as well. As illustrated in Figure 9 (dashed box), the sign of the ECCD couplet can be predicted by analyzing the substituent on the chiral center that bears the largest group.

As can be seen from Table 4, a variety of substituents and functional groups produced the expected results. Also, the presence of other potential coordinating groups such as esters (Table 4, compounds **13**, **16**, **18**, and **22**) or acetonide (**23**) did not interfere with the complexation of the substrates with tweezer **3**. As expected, *threo* diamines produced much higher ECCD amplitudes than diols due to their stronger binding with tweezer **3**. Interestingly, tweezer **3** was capable of binding diepoxide **27** and produced the expected ECCD spectrum based on the binding mode explained above (see Supporting Information). The absolute stereochemical determination of epoxy alcohols via binding of the epoxide will be reported in due course.

As with the *erythro* compounds, the CD for *threo* systems was measured at 0 °C in order to improve the observed ECCD amplitudes. Although the use of MCH as the solvent (traditionally used as the preferred solvent for ECCD measurements with Zn tweezers) produced ECCD spectra with large amplitudes, it was observed that hexane in most cases would increase the strength of the signal. For instance, the two weakest performing *threo* substrates **14** (A = +33) and **18** (A = +20) exhibited much larger ECCD amplitudes (+62 and +76, respectively) in hexane. As described above, the proposed binding of porphyrin tweezer **3** with *erythro* and *threo* systems is similar, in which

each porphyrin binds the coordinating functional group opposite the largest substituent on the chiral center. It should be noted that in all cases discussed thus far the nature of the acyclic system could lead to a number of rotomers upon complexation (Figures 7 and 9 only depict the rotomer believed to lead to the observed ECCD spectra for *erythro* and *threo* systems, respectively). It is difficult to predict whether or not the conformation of the complexed guest molecules retains the lowest energy conformation of unbound molecules (such as those depicted in Figure 1) since complexation with the large porphyrin tweezer can lead to compensating interactions with an overall effect of the guest system adopting a higher energy conformation.

NMR experiments have not been useful in assigning the conformation of the bound guest molecules since aggregation of the Zn-TPFP porphyrin tweezer is observed at concentrations necessary for observing NMR signals (based on our observations, the fluorinated porphyrin has a much higher tendency for aggregation as compared to the nonfluorinated porphyrin). At the same time, the solutions used for NMR analysis (10^{-3}–10^{-4} M) were found to be ECCD silent. In solvents that reduced the level of aggregations, such as $CHCl_3$, CH_2Cl_2, and CH_3CN, ECCD was absent upon binding with the chiral guests. This is presumably due to the high Lewis acidity of the Zn-TPFP porphyrin tweezer and its ability to interact with solvents more polar than hydrocarbons. Computational minimizations of the complexed system, albeit at a low level of theory due to the large size of the complex, agree with the proposed models (see Supporting Information for details and alternate conformations of the bound guests leading to the expected ECCD spectra). In summary, the conformations of the bound chiral guest molecules that are depicted in Figures 7 and 9 to yield the observed ECCD spectra are speculative; however, the mnemonic that is derived from these observations consistently provides the anticipated ECCD spectra and can be used reliably.

Comparison between TPFP Tweezer and TPP Tweezer. Initially, this project was pursued based on the supposition that steric differentiation of each chiral site bound to the porphyrin tweezer will result in an induced helicity that is observable as an ECCD signal. Although, as described above, this has come to fruition, the initial attempts were discouraging due to the fact that different structures with the same chirality produced differing ECCD signs or none at all. It should be noted that initially the Zn−TPP tweezer was utilized, and it became apparent that weak binding of substrates potentially contributes to a number of different, energetically close conformations of the complex. As we have documented above, the solution to this problem was to increase the binding of the guest molecules with the host porphyrin tweezer by increasing the Lewis acidity of the zincated porphyrins. Functional comparison of the porphyrin tweezers (Zn−TPP **1** vs Zn−TPFP **3**) in deducing the absolute stereochemistry of a number of *threo* and *erythro* diols is provided in Table 5. The measurements were taken in hexane to ensure maximum binding. As was described above and shown in Table 5, the predicted sign for ECCD matched the observed spectra for all substrates tested with Zn-TPFP tweezer **3**. However, among *erythro* diols only **8** and **9** yielded observable ECCD signals with Zn-TPP tweezer **1**, albeit with lower amplitudes as compared to those obtained with Zn-TPFP tweezer **3**. Moreover, diol **8** did not yield the expected ECCD.

Table 5. Tweezer **1**[a] Bound *erythro* and *threo* 1,2-Diols[b]

	chiral substrates[d]	predicted sign	λ nm, (Δε)	A
8 *R,S*		+	430 (-9) 414 (+11)	-20
9 *S,R*	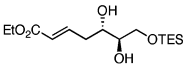	-	426 (-6) 416 (+10)	-16
14 *R,R*		+	No ECCD	
15 *R,R*		+	429 (+17) 414 (-8)	+25
16 *R,R*	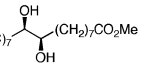	+	429 (+34) 416 (-18)	+52
17 *S,S*	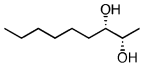	-	No ECCD	
18 *S,S*	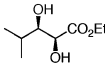	+	No ECCD	
19[c] *S,S*	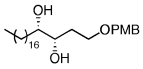	-	426 (+42) 414 (-24)	+66
20 *S,S*		-	No ECCD	

[a] 1 μM tweezer **1** concentration was used for all measurements except for **8** and **9** (2 μM). [b] Tweezer/substrate ratio, 1:40. [c] Tweezer/substrate ratio, 1:100. [d] Hexane was used as solvent for all CD measurements.

All other *erythro* diols tested did not exhibit an ECCD signal. As shown in Table 5, many *threo* diols were also ECCD silent in the presence of Zn-TPP tweezer **1**. From those that did provide a signal, compounds **15** and **16**, which led to the highest amplitudes among the diols with Zn-TPFP tweezer **3**, showed much weaker signals when bound with Zn-TPP tweezer **1**. Other *threo* diols such as **19** generated signals with signs that are opposite to the predicted model.

It seems reasonable to conclude that the binding affinity of host−guest complexes used in absolute stereochemical determinations must be considered, especially if weak CD signals and/or inconsistent signs are obtained. In this case, with the use of the electron deficient Zn-TPFP tweezer, the binding of the diols is sufficiently strong to produce consistent ECCD spectra leading to a general approach for absolute stereochemical determination of 1,2-systems.

Conclusion

We demonstrate the prompt microscale determination of absolute configurations for *threo* and most importantly the often difficult to determine *erythro* diols, amino alcohols, and diamines utilizing the porphyrin tweezer methodology. Conservative estimates are that 1 nmol of material is required for analysis of diamines and amino alcohols and 40 nmol are needed for analysis of diols (along with 1 nmol of porphyrin tweezer for each analysis). To the best of our knowledge this is the first routine method that addresses the absolute stereochemical determination of *erythro* compounds. This methodology also requires no derivatizations, which is often used for the absolute stereochemical determination of *threo* compounds. Utility of the fluorinated tweezer **3** for binding with other functional groups is under investigation.

Acknowledgment. Generous support was provided by the NSF CAREER (CHE-0094131) grant.

Supporting Information Available: Experimental procedures for synthesis of porphyrin tweezer **3**, diols **6**−**10**, **13**−**19**, **21**, **23**, **27**; Spectra data and optical purity of all the synthesized diols; ECCD data for seven enantiomers of *threo* substrates **13**−**16**, **22**, **25**, **26**; Molecular modeling of TPFP tweezer complexed with **12**, **15**, and diepoxide **27**. This material is available free of charge via the Internet at http://pubs.acs.org

JA0752639